Available online at www.sciencedirect.com
SCIENCE DIRECT®
International Journal of Solids and Structures 43 (2006) 5570–5580
INTERNATIONAL JOURNAL OF SOLIDS and STRUCTURES
www.elsevier.com/locate/ijsolstr

Exact solutions for functionally graded pressure vessels in a uniform magnetic field

H.L. Dai [a,*], Y.M. Fu [a], Z.M. Dong [b]

[a] Department of Engineering Mechanics, Hunan University, Changsha 410082, Hunan Province, People's Republic of China
[b] Nanjing Institute of Astronomical Optics and Technology, Chinese National Astronomical Observatories, CAS, Nanjing 210042, People's Republic of China

Received 4 May 2005
Available online 2 November 2005

Abstract

Analytical studies for magnetoelastic behavior of functionally graded material (FGM) cylindrical and spherical vessels placed in a uniform magnetic field, subjected to internal pressure are presented. Exact solutions for displacement, stress and perturbation of magnetic field vector in FGM cylindrical and spherical vessels are determined by using the infinitesimal theory of magnetoelasticity. The material stiffness and magnetic permeability obeying a simple power law are assumed to vary through the wall thickness and Poisson's ratio is assumed constant. Stresses and perturbation of magnetic field vector distributions depending on an inhomogeneous constant are compared with those of the homogeneous case and presented in the form of graphs. The inhomogeneous constant, which includes continuously varying volume fraction of the constituents, is empirically determined. The values used in this study are arbitrary chosen to demonstrate the effect of inhomogeneity on stresses and perturbation of magnetic field vector distributions.

Keywords: FGM; Magnetoelasticity; Perturbation of magnetic field vector

1. Introduction

The mechanical properties of cylindrical and spherical structures made of functionally graded material (FGM) vary continuously in the macroscopic sense from on surface to the other. This is achieved by gradually varying the volume fraction of the constituent materials in the manufacturing process. FGMs are composite materials intentionally designed so that they possess desirable properties for some specific applications.

Recently there has been growing interest in materials deliberately fabricated so that their mechanical properties vary continuously in space on the macroscopic scale. Previous studies on the subject considered FGM including those, for example, by Tanigawa (1995), Horgan and Chan (1998, 1999), Yang (2000), Rooney and

* Corresponding author.
E-mail addresses: hldai520@sina.com, hldai520@sjtu.edu.cn (H.L. Dai).

0020-7683/$ - see front matter © 2005 Elsevier Ltd. All rights reserved.
doi:10.1016/j.ijsolstr.2005.08.019

Nomenclature

$\vec{U}, u$	displacement vector and radial displacement [m]
E_0, v	elastic constant and Poisson ratio
σ_r, σ_θ	components of stresses [N/m^2]
ρ, t	mass density [kg/m^3] and time variable [s]
r	radial variable [m]
$\vec{H}$	magnetic intensity vector
$\vec{h}$	perturbation of magnetic field vector
$\vec{J}$	electric current density vector
$\vec{e}$	perturbation of magnetic field vector
μ_0	magnetic permeability [H/m]
f_z, f_ϕ	Lorentz's force [kg/m^2 s^2]
a, R	inner and outer radii of the FGM hollow cylinder and the FGM hollow sphere [m]

Ferrari (2001), where additional references can be found. A few studies had addressed this. Liu et al. (1991, 1992) used strip element method to deal with an FGM plate. The elastic problem of thick-walled tubes of a functionally graded material under internal pressure in the case of plane strain had been studied by Fukui and Yamanaka (1992). Durodola and Adlington (1996) presented the use of numerical methods to assess the effect of various forms of gradation of material properties to control deformation and stresses in rotating axisymmetric components such as disks and rotors. Nadeau and Ferrari (1999) presented a one-dimensional thermal stress analysis of a transversely isotropic layer that is inhomogeneous in its thickness. The works concerned with the stress analysis of cylindrical structural elements involve finite elements and other numerical techniques due to the nature of functions chosen to describe the inhomogeneous properties (Loy et al., 1999; Salzar, 1995). Using the infinitesimal theory of elasticity, Tutuncu and Ozturk (2001) obtained the closed-form solutions for stresses and displacements in functionally graded cylindrical and spherical vessels subjected to internal pressure. However, investigations on the exact solutions for FGM pressure vessels in a uniform magnetic field have not been found in the literature.

The present paper is, upon employing simplifying assumptions, to present to the technical community in the field simple, tractable closed-form solutions in FGM cylindrical and spherical vessels. The aim of this research is to understand the effect of the volumetric ratio of constituents and porosity on magnetoelastic stresses and perturbation of magnetic field vector and to design the optimum FGM cylindrical and spherical vessels.

It is assumed that the material is isotropic with constant Poisson's ratio and radially varying elastic modulus and magnetic permeability are, respectively, approximated by $E(r) = E_0 r^\beta$ and $\mu(r) = \mu_0 r^\beta$, the similar assumption can be found in previous studies (Ye et al., 2001; Tarn, 2001; Wu et al., 2003). Since r is away from zero and ranges in (a, R) by adjusting the constants E_0, μ_0 and β, it is possible to obtain physically meaningful results. The range $-2 \leqslant \beta \leqslant 2$ to be used in the present study covers all the values of coordinate exponent encountered in the references cited earlier. However, these values for β do not necessarily represent a certain material. Various β values are used to demonstrate the effect of inhomogeneity on the stress and perturbation of magnetic field vector distributions.

2. Basic formulations and solutions

The stress and perturbation of magnetic field vector distributions in FGM cylindrical and spherical pressure vessels will be calculated. The radial coordinate $\bar{r}$ and the displacement $\bar{u}$ are normalized as $r = \bar{r}/R$ and $u = \bar{u}/R$ where R is the outer radii of the FGM cylindrical and spherical vessels. The stiffness and magnetic permeability are assumed to vary as $E(r) = E_0 r^\beta$ and $\mu(r) = \mu_0 r^\beta$ through the wall thickness, respectively. Here, E_0 is the stiffness at the outer surface ($r = 1$), μ_0 is the magnetic permeability at the outer surface ($r = 1$) and β is the inhomogeneous constant determined empirically.

2.1. Cylindrical vessel

A long, FGM hollow cylinder with perfect conductivity placed in a uniform magnetic field $\vec{H}(0,0,H_z)$ is shown in Fig. 1, letting the cylindrical coordinates of any representative point be (r,θ,z). For the axisymmetry plain strain assumption problem, the constitutive relations are

$$\sigma_r = c_{11}\frac{\partial u}{\partial r} + c_{12}\frac{u}{r}, \qquad \sigma_\theta = c_{12}\frac{\partial u}{\partial r} + c_{11}\frac{u}{r} \tag{1a, b}$$

where

$$c_{11} = \left[\frac{E_0(1-v)}{(1+v)(1-2v)}\right]r^\beta, \qquad c_{12} = \left[\frac{E_0 v}{(1+v)(1-2v)}\right]r^\beta \tag{2}$$

The boundary conditions are expressed as

$$\sigma_r(a/R) = -p, \qquad \sigma_r(1) = 0 \tag{3}$$

Assuming that the magnetic permeability, μ_0, at the outer surface ($r = 1$) of the FGM cylindrical vessel equals the magnetic permeability of the medium around it and omitting displacement electric currents, the governing electrodynamic Maxwell equations (Kraus, 1984; Dai and Wang, 2004) for a perfectly conducting, elastic body are given by

$$\vec{J} = \nabla \times \vec{h}, \qquad \nabla \times \vec{e} = -\mu(r)\frac{\partial \vec{h}}{\partial t}, \qquad \text{div}\ \vec{h} = 0, \qquad \vec{e} = -\mu(r)\left(\frac{\partial \vec{U}}{\partial t} \times \vec{H}\right),$$
$$\vec{h} = \nabla \times (\vec{U} \times \vec{H}) \tag{4}$$

Applying an initial magnetic field vector $\vec{H}(0,0,H_z)$ in cylindrical coordinate (r,θ,z) system to Eq. (4), yields

$$\vec{U} = (u,0,0), \qquad \vec{e} = -\mu(r)\left(0, H_z\frac{\partial u}{\partial t}, 0\right), \tag{5a}$$

$$\vec{h} = (0,0,h_z), \qquad \vec{J} = \left(0, -\frac{\partial h_z}{\partial r}, 0\right), \qquad h_z = -H_z\left(\frac{\partial u}{\partial r} + \frac{u}{r}\right) \tag{5b}$$

The electromagnetic dynamic equation of the FGM hollow cylinder, in absence of body forces, is expressed as

$$\frac{\partial \sigma_r}{\partial r} + \frac{\sigma_r - \sigma_\theta}{r} + f_z = 0 \tag{6}$$

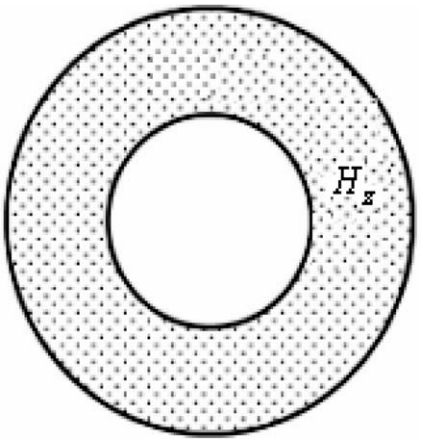

Fig. 1. The geometry of a FGM hollow cylinder in a uniform magnetic field H_z.

where f_z is defined as Lorentz's force (Kraus, 1984; Dai and Wang, 2004), which may be written as

$$f_z = \mu(r)(\vec{J} \times \vec{H}) = \mu_0 H_z^2 \frac{\partial}{\partial r}\left(r^\beta \frac{\partial u}{\partial r} + r^\beta \frac{u}{r}\right) \tag{7}$$

Substituting Eqs. (1), (2) and (7) into Eq. (6), yields

$$r^2 \frac{\partial^2 u}{\partial r^2} + (1+\beta) r \frac{\partial u}{\partial r} + (\lambda\beta - 1)u = 0 \tag{8}$$

where

$$\lambda = \frac{v + \mu_0 H_z^2 (1+v)(1-2v)}{1 - v + \mu_0 H_z^2 (1+v)(1-2v)} \tag{9}$$

Eq. (8) is the familiar Euler–Cauchy equation with the characteristic equation (10)

$$m^2 + \beta m + (\lambda\beta - 1) = 0 \tag{10}$$

the characteristic equation's roots are

$$m_1 = \frac{1}{2}(-\beta - \sqrt{4 + \beta^2 - 4\beta\lambda}) \tag{11a}$$

$$m_2 = \frac{1}{2}(-\beta + \sqrt{4 + \beta^2 - 4\beta\lambda}) \tag{11b}$$

For any stable materials, we always have $c_{12} < c_{11}$ which indicates that the discriminant of Eq. (10) is always greater than zero. That is to say, m_1 and m_2 are real and distinct. The solution to Eq. (8) is

$$u = Ar^{m_1} + Br^{m_2} \tag{12}$$

By virtue of Eq. (12), the expressions of the radial, circumferential stresses and perturbation of magnetic field vector of the FGM cylindrical vessel are derived as follows:

$$\sigma_r = \frac{E_0}{(1+v)(1-2v)}\{[(1-v)m_1 + v]Ar^{m_1+\beta-1} + [(1-v)m_2 + v]Br^{m_2+\beta-1}\} \tag{13a}$$

$$\sigma_\theta = \frac{E_0}{(1+v)(1-2v)}[(1 - v + vm_1)Ar^{m_1+\beta-1} + (1 - v + vm_2)Br^{m_2+\beta-1}] \tag{13b}$$

$$h_z = -H_z[(m_1+1)Ar^{m_1-1} + (m_2+1)Br^{m_2-1}] \tag{13c}$$

The constants A and B are determined from the boundary conditions (3)

$$A = -\frac{p\left(\frac{a}{R}\right)^{1-\beta}(1+v)(1-2v)}{E_0\left[\left(\frac{a}{R}\right)^{m_1} - \left(\frac{a}{R}\right)^{m_2}\right][v + (1-v)m_1]} \tag{14a}$$

$$B = \frac{p\left(\frac{a}{R}\right)^{1-\beta}(1+v)(1-2v)}{E_0\left[\left(\frac{a}{R}\right)^{m_1} - \left(\frac{a}{R}\right)^{m_2}\right][v + (1-v)m_2]} \tag{14b}$$

So Eqs. (13) can be written as

$$\sigma_r = -\frac{p\left(\frac{a}{R}\right)^{1-\beta}(r^{m_1} - r^{m_2})r^{\beta-1}}{\left(\frac{a}{R}\right)^{m_1} - \left(\frac{a}{R}\right)^{m_2}} \tag{15a}$$

$$\sigma_\theta = \frac{p\left(\frac{a}{R}\right)^{1-\beta}(\eta_1 - \eta_2)}{\left[\left(\frac{a}{R}\right)^{m_1} - \left(\frac{a}{R}\right)^{m_2}\right][m_1(v-1) - v][m_2(v-1) - v]} \tag{15b}$$

$$h_z = H_z \frac{p\left(\frac{a}{R}\right)^{1-\beta}(1+v)(1-2v)}{E_0\left[\left(\frac{a}{R}\right)^{m_1} - \left(\frac{a}{R}\right)^{m_2}\right]}\left\{\frac{(m_1+1)r^{m_1-1}}{[v + (1-v)m_1]} - \frac{(m_2+1)r^{m_2-1}}{[v + (1-v)m_2]}\right\} \tag{15c}$$

where

$$\eta_1 = r^{m_1}[m_2(v-1)-v][1+(m_1-1)v] \tag{16a}$$

$$\eta_2 = r^{m_2}[m_1(v-1)-v][1+(m_2-1)v] \tag{16b}$$

2.2. Spherical vessel

A FGM hollow sphere with perfect conductivity placed in a uniform magnetic field $\vec{H}(0,0,H_\phi)$ is shown in Fig. 2, letting the spherical coordinates of any representative point be (r,θ,ϕ), the constitutive relations are (Sinha, 1962; Dai and Wang, 2005)

$$\sigma_r = c_{11}\frac{\partial u}{\partial r} + 2c_{12}\frac{u}{r}, \qquad \sigma_\theta = c_{12}\frac{\partial u}{\partial r} + (c_{11}+c_{12})\frac{u}{r} \tag{17a, b}$$

Omitting displacement electric currents, the governing electrodynamic Maxwell equations (Kraus, 1984) for a perfectly conducting, elastic body are given by

$$\vec{J} = \mathrm{Curl}\,\vec{h}, \qquad \mathrm{Curl}\,\vec{e} = -\mu\frac{\partial \vec{h}}{\partial t}, \qquad \mathrm{div}\,\vec{h} = 0, \qquad \vec{e} = -\mu\left(\frac{\partial \vec{U}}{\partial t}\times\vec{H}\right),$$

$$\vec{h} = \mathrm{Curl}(\vec{U}\times\vec{H}) \tag{18}$$

Applying an initial magnetic field vector $\vec{H}(0,0,H_\phi)$ in spherical coordinate (r,θ,ϕ) system to Eq. (18), yields

$$\vec{U} = (u,0,0), \qquad \vec{e} = -\mu(r)\left(0, H_\phi\frac{\partial u}{\partial t}, 0\right) \tag{19a}$$

$$\vec{h} = (0,0,h_\phi), \qquad \vec{J} = \left(0, -\frac{\partial h_\phi}{\partial r}, 0\right), \qquad h_\phi = -H_\phi\left(\frac{\partial u}{\partial r}+\frac{2u}{r}\right) \tag{19b}$$

The electromagnetic dynamic equation of the FGM hollow sphere, in absence of body forces, is expressed as

$$\frac{\partial \sigma_r}{\partial r} + \frac{2(\sigma_r-\sigma_\theta)}{r} + f_\phi = 0 \tag{20}$$

where f_ϕ is defined as Lorentz's force (Kraus, 1984), which may be written as

$$f_\phi = \mu(r)(\vec{J}\times\vec{H}) = \mu_0 H_\phi^2\frac{\partial}{\partial r}\left(r^\beta\frac{\partial u}{\partial r} + r^\beta\frac{2u}{r}\right) \tag{21}$$

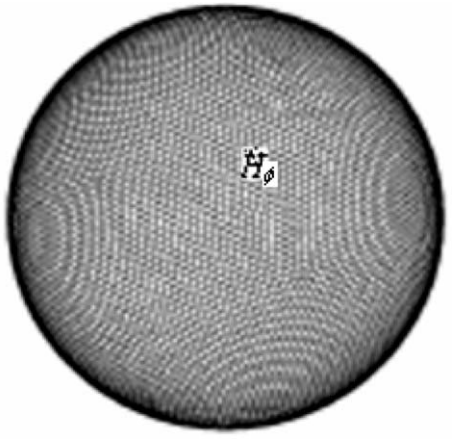

Fig. 2. The geometry of FGM hollow sphere in a uniform magnetic filed H_ϕ.

Substituting Eqs. (2), (17) and (21) into Eq. (20), yields

$$r^2\frac{\partial^2 u}{\partial r^2}+(2+\beta)r\frac{\partial u}{\partial r}+2(\lambda\beta-1)u=0 \tag{22}$$

where

$$\Delta=\frac{v+\mu_0 H_\phi^2(1+v)(1-2v)}{1-v+\mu_0 H_\phi^2(1+v)(1-2v)} \tag{23}$$

Eq. (22) is the familiar Euler–Cauchy equation with the characteristic equation (24)

$$s^2+(\beta+1)s+2(\Delta\beta-1)=0 \tag{24}$$

the characteristic equation's roots are

$$s_1=\frac{1}{2}(-1-\beta-\sqrt{9+2\beta+\beta^2-8\beta\Delta}) \tag{25a}$$

$$s_2=\frac{1}{2}(-1-\beta+\sqrt{9+2\beta+\beta^2-8\beta\Delta}) \tag{25b}$$

Here also, only real, distinct roots will be considered. The solution is

$$u=Cr^{s_1}+Dr^{s_2} \tag{26}$$

By virtue of Eq. (26), the expressions of the radial, circumferential stresses and perturbation of magnetic field vector of the FGM spherical vessel are derived as follows:

$$\sigma_r=\frac{E_0}{(1+v)(1-2v)}\{[(1-v)s_1+2v]Cr^{s_1+\beta-1}+[(1-v)s_2+2v]Dr^{s_2+\beta-1}\} \tag{27a}$$

$$\sigma_\theta=\frac{E_0}{(1+v)(1-2v)}[(1+vs_1)Cr^{s_1+\beta-1}+(1+vs_2)Dr^{s_2+\beta-1}] \tag{27b}$$

$$h_z=-H_z[(s_1+1)Cr^{s_1-1}+(s_2+1)Dr^{s_2-1}] \tag{27c}$$

The constants C and D are determined from the boundary conditions Eq. (3)

$$C=-\frac{p\left(\frac{a}{R}\right)^{1-\beta}(1+v)(1-2v)}{E_0\left[\left(\frac{a}{R}\right)^{s_1}-\left(\frac{a}{R}\right)^{s_2}\right][2v+(1-v)s_1]} \tag{28a}$$

$$D=-\frac{p\left(\frac{a}{R}\right)^{1-\beta}(1+v)(1-2v)}{E_0\left[\left(\frac{a}{R}\right)^{s_1}-\left(\frac{a}{R}\right)^{s_2}\right][2v+(1-v)s_2]} \tag{28b}$$

So Eqs. (27) can be rewritten as

$$\sigma_r=-\frac{p\left(\frac{a}{R}\right)^{1-\beta}(r^{s_1}-r^{s_2})r^{\beta-1}}{\left(\frac{a}{R}\right)^{s_1}-\left(\frac{a}{R}\right)^{s_2}} \tag{29a}$$

$$\sigma_\theta=\frac{p\left(\frac{a}{R}\right)^{1-\beta}(\delta_1-\delta_2)}{\left[\left(\frac{a}{R}\right)^{s_1}-\left(\frac{a}{R}\right)^{s_2}\right][s_1(v-1)-2v][s_2(v-1)-2v]} \tag{29b}$$

$$h_z=H_z\frac{p\left(\frac{a}{R}\right)^{1-\beta}(1+v)(1-2v)}{E_0\left[\left(\frac{a}{R}\right)^{s_1}-\left(\frac{a}{R}\right)^{s_2}\right]}\left\{\frac{s_1+1}{[2v+(1-v)s_1]}r^{s_1-1}-\frac{s_2+1}{[2v+(1-v)s_2]}r^{s_2-1}\right\} \tag{29c}$$

where

$$\delta_1=r^{s_1-1}[s_2(v-1)-2v]\{v+r^\beta[1+(s_1-1)v]\} \tag{30a}$$

$$\delta_2=r^{s_2-1}[s_1(v-1)-2v]\{v+r^\beta[1+(s_2-1)v]\} \tag{30b}$$

Stresses and perturbation of magnetic field vector for the FGM pressure vessels will be compared with those for the homogeneous ones. The well-known stresses and perturbation of magnetic field vector expressions for the homogeneous vessels under internal pressure can easily be obtained by setting $\beta = 0$ in the FGM case. It should also be noted that no Poisson's ratio is presented in the homogeneous case whereas it is clearly noticed in the FGM case along with the inhomogeneous constant.

3. Numerical results and discussion

Example 1. The results are presented for $a/R = 0.5$ and $v = 0.3$. Figs. 3–5 show the radial stress, circumferential stress and perturbation of magnetic field vector distributions in the FGM cylindrical vessel, respectively. From the curve of Figs. 3 and 4, one knows, a positive β means increasing stiffness in the radial direction for $0.5 \leqslant r \leqslant 1$ (at $r = 1$, the limit of normalized stress is calculated). Under internal pressure alone, more stiffness is needed near the inner surface to better withstand the applied pressure. Thus, decreasing the stiffness in the radial direction increases stresses with respect to the homogeneous case. The converse is obviously true; having higher stiffness near the inner surface carries the applied pressure leading to decreasing stresses through the wall thickness. Fig. 5 depicts the distribution of perturbation of magnetic field vector, from the curves in Fig. 5, it is seen that the variation of perturbation of magnetic field vector is different that in Figs. 3 and 4, the magnitude of value of perturbation of magnetic field vector is become gradually small from inner wall to outer wall of the FGM cylindrical vessel. The same FGM spherical vessel (i.e., $a/R = 0.5$ and $v = 0.3$) is

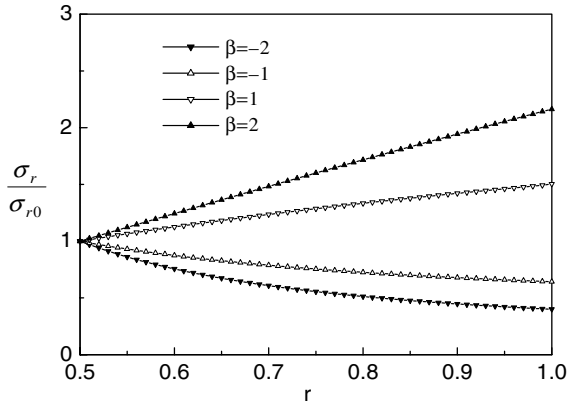

Fig. 3. Radial stress distribution in FGM hollow cylinder, where $a/R = 0.5$.

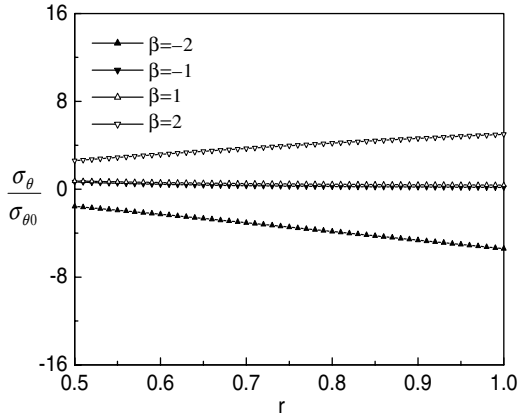

Fig. 4. Circumferential stress distribution in FGM hollow cylinder, where $a/R = 0.5$.

observed in Figs. 6 and 7. Comparing Figs. 6 and 3, it is seen easily that radial stress distributions is nearly the same. It is seen easily from Figs. 4 and 7 that the circumferential stress distributions have the same trend, but

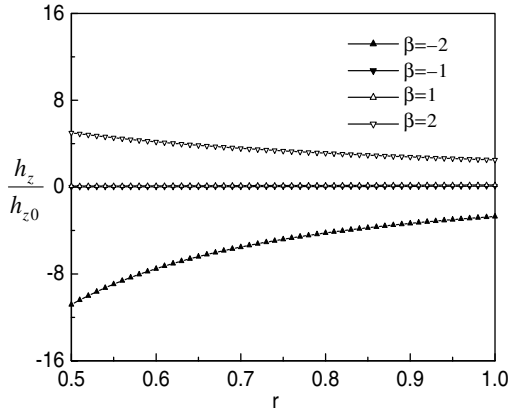

Fig. 5. The perturbation of magnetic field vector distribution in FGM hollow cylinder, where $a/R = 0.5$.

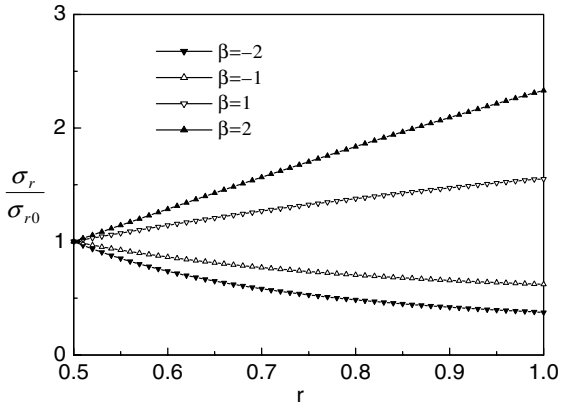

Fig. 6. Radial stress distribution in FGM hollow sphere, where $a/R = 0.5$.

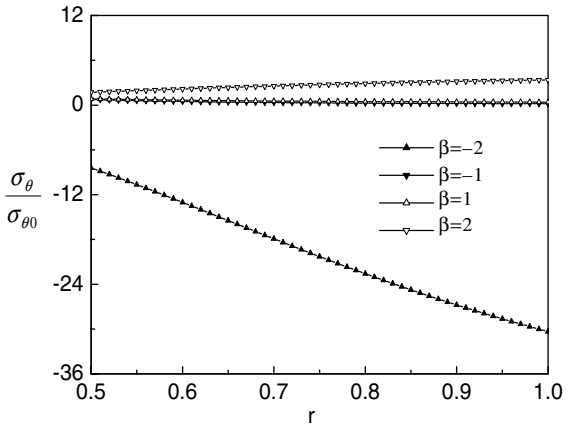

Fig. 7. Circumferential stress distribution in FGM hollow sphere, where $a/R = 0.5$.

the magnitude of value of circumferential stress in the FGM spherical vessel is larger than that of FGM cylindrical vessel.

Example 2. The results are presented for $a/R = 0.9$ and $v = 0.3$. The same non-dimensional quantities are taken as Example 1. Figs. 8–10 show the radial stress, circumferential stress and perturbation of magnetic field

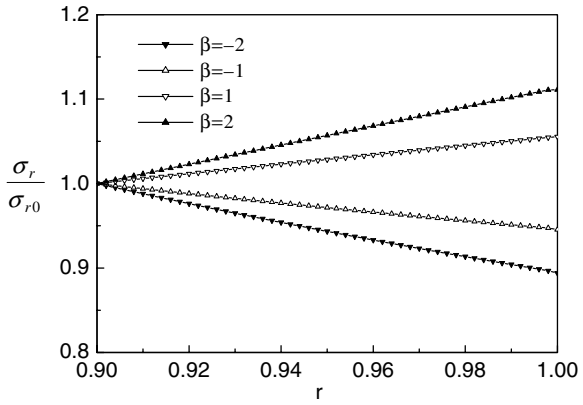

Fig. 8. Radial stress distribution in FGM hollow cylinder, where $a/R = 0.9$.

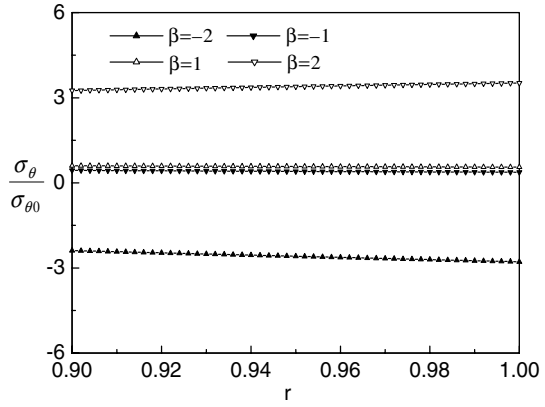

Fig. 9. Circumferential stress distribution in FGM hollow cylinder, where $a/R = 0.9$.

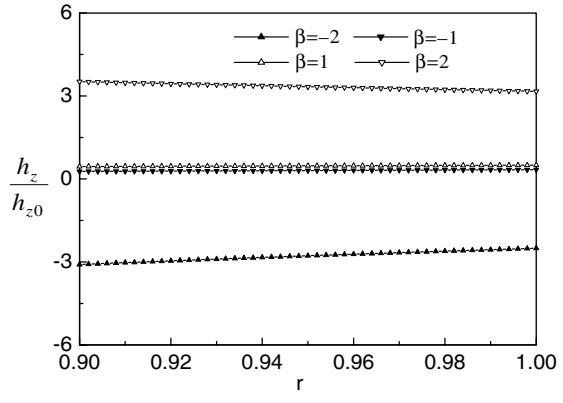

Fig. 10. The perturbation of magnetic field vector distribution in FGM hollow cylinder, where $a/R = 0.9$.

vector distributions in the FGM cylindrical vessel, respectively. Comparing Figs. 8 and 3, one found, the curves are the same trend as the structure is difference. It is seen easily from Figs. 9 and 4 that the trend of curve becomes the slower as the structures takes thinner. The same trend in perturbation of magnetic field vector of FGM cylindrical vessels is observed by comparing Figs. 5 with 10.

4. Conclusion

1. By means of the infinitesimal theory of magnetoelasticity, exact solutions for FGM cylindrical and spherical vessels in a uniform magnetic field, subjected to internal pressure are obtained. The inhomogeneous constant presented in the present study is useful parameter from a design point of view in that it can be tailored for specific applications to control the stress and perturbation of magnetic field vector distributions.
2. Numerical results show that the gradient index β has a great effect on the magnetoelastic stress and perturbation of magnetic field vector. For example, a negative β will yield compressive radial stress at the inner surface and tensile radial stress at the outer surface, while a positive β gives a contrary result. Thus by selecting a proper value of β, it is possible for engineers to design FGM cylindrical and spherical vessels that can meet some special requirements.
3. Although this paper considers the case in which the material constants are of power functions in the radial variable, the technique is applicable to other material inhomogeneity.

Acknowledgements

The authors appreciate the valuable comments from the reviewers.

References

Dai, H.L., Wang, X., 2004. Dynamic responses of piezoelectric hollow cylinders in an axial magnetic field. International Journal of Solids and Structures 41, 5231–5246.

Dai, H.L., Wang, X., 2005. Transient wave propagation in piezoelectric hollow spheres subjected to thermal shock and electric excitation. Structural Engineering and Mechanics 19 (4), 441–457.

Durodola, J.F., Adlington, J.E., 1996. Functionally graded material properties for disks and rotors. In: Proceedings of the 1996 First International Conference on Ceramic and Metal Matrix Composites, San Sebastian, Spain.

Fukui, Y., Yamanaka, N., 1992. Elastic analysis for thick-walled tubes of functionally graded material subjected to internal pressure. JSME International Journal, Series 1: Solid Mechanics, Strength of Materials 35, 379.

Horgan, C.O., Chan, A.M., 1998. Torsion of functionally graded isotropic linearly elastic bars. Journal of Elasticity 52, 181–199.

Horgan, C.O., Chan, A.M., 1999. Stress response of functionally graded isotropic linearly elastic rotating disks. Journal of Elasticity 55, 219–230.

Kraus, J.D., 1984. Electromagnetic. McGraw-Hill, Inc., USA.

Liu, G.R., Tani, J., 1992. SH surface waves in functionally gradient piezoelectric material plates. Transactions of the Japan Society of Mechanical Engineers A 58 (547), 504–507.

Liu, G.R., Tani, J., Ohyoshi, T., 1991. Lamb waves in a functionally gradient material plates and its transient response. Part1: Theory; Part 2: Calculation results. Transactions of the Japan Society of Mechanical Engineers 57A (535), 131–142.

Loy, C.T., Lam, K.Y., Reddy, J.N., 1999. Vibration of functionally graded cylindrical shells. International Journal of Mechanical Sciences 41 (3), 309–324.

Nadeau, J.C., Ferrari, M., 1999. Microstructural optimization of a functionally graded transversely isotropic layer. Mechanics of Materials 31, 637–651.

Rooney, F., Ferrari, M., 2001. Tension, bending, and flexure of functionally graded cylinders. International Journal of Solids and Structures 38, 413–421.

Salzar, R.S., 1995. Functionally graded metal matrix composite tubes. Computer and Engineering 5 (7), 891–900.

Sinha, D.K., 1962. Note on the radial deformation of a piezoelectric polarized spherical shell with symmetrical temperature distribution. Journal of Acoustical Society of America 34, 1073–1075.

Tanigawa, Y., 1995. Some basic thermoelastic problems for nonhomogeneous structural materials. ASME Applied Mechanics Review 48, 287–300.

Tarn, J.Q., 2001. Exact solutions for functionally graded anisotropic cylinders subjected to thermal and mechanical loads. International Journal of Solids and Structures 38, 8189–8206.

Tutuncu, N., Ozturk, M., 2001. Exact solutions for stresses in functionally graded pressure vessels. Composite: Part B 32, 683–686.

Wu, X.H., Shen, Y.P., Chen, C.Q., 2003. An exact solution for functionally graded piezothermoelastic cylindrical shell as sensors or actuators. Materials Letters 57, 3532–3542.

Yang, Y.Y., 2000. Time-dependent stress analysis in functionally graded materials. International Journal of Solids and Structures 37, 7593–7608.

Ye, G.R., Chen, W.Q., Cai, J.B., 2001. A uniformly heated functionally graded cylindrical shell with transverse isotropy. Mechanics Research Communication 28 (5), 535–542.